FOREX Publication
Open Access | Rapid and quality publishing

International Journal of
Electrical and Electronics Research (IJEER)
Research Article | Volume 12, Issue 2 | Pages 639-646 | e-ISSN: 2347-470X

Multi Renewable Source System Stabilization using ANFIS Controller for Energy Storage Module

Ch. Laxmi[1*], Dr. M. Narendra Kumar[2] and Dr. Rajendra Kumar Khadanga[3]

[1]*Centurion University of Technology and Management, Odisha, India; laxmichanumalla@gmail.com*
[2] *Kasireddy Narayanreddy College of Engineering & Research, Hyderabad, India; narendrakumar_maddargi@yahoo.com*
[3] *Centurion University of Technology and Management, Odisha, India; rajendra.khadanga@cutm.ac.in*

***Correspondence:** Ch. Laxmi; laxmichanumalla@gmail.com

ABSTRACT- When a system is operated with multiple renewable sources connected to the same bus, several power quality issues are raised which may damage the devices connected to it. The issues like DC voltage regulation, harmonics in the AC voltages and ripple in the currents of the devices might be a major concern in the system. This compromising power quality can be improved by integrating advanced adaptive controller into the system for stable voltages. For this a multi renewable source system is considered including PMSG wind farm, FC module, PV source and a battery unit energy storage module. The battery unit is a mandatory module which maintains the power exchange and DC link voltage stability. The fuel cell module is a backup unit to the system when the battery unit fails. In normal operating conditions the battery unit has the majority control over the system. Therefore, the controller of the battery unit is updated with an ANFIS control structure improving the DC link voltage stabilization, helps to mitigate harmonics on the AC side. A relative analysis is done with traditional PI controller and proposed ANFIS controller generating comparative parameters and graphs using MATLAB software Simulink tools. The stability of the system is validated by operating it in different conditions, testing the ability of the proposed controller.

Keywords: PMSG (Permanent Magnet Synchronous Motor), FC (Fuel Cell), PV (Photo Voltaic), ANFIS (Adaptive Neuro Fuzzy Inference System), PI (Proportional Integral), MATLAB (Matrix Laboratory).

ARTICLE INFORMATION

Author(s): Ch. Laxmi, Dr. M. Narendra Kumar and Dr. Rajendra Kumar Khadanga;

Received: 19/03/2024; **Accepted**: 28/05/2024; **Published**: 25/06/2024;
e-ISSN: 2347-470X;
Paper Id: IJEER 1903-14;
Citation: 10.37391/IJEER.120241
Webpage-link:
https://ijeer.forexjournal.co.in/archive/volume-12/ijeer-120241.html

Publisher's Note: FOREX Publication stays neutral with regard to Jurisdictional claims in Published maps and institutional affiliations.

1. INTRODUCTION

The From past few years there has been an exponential increase in interest on research of renewable sources. These renewable sources are considered to be an alternative to the present fossil fuel power generation [1]. As the alternative energy sources generated power using natural resources like solar irradiation, wind, biogas, tidal etc., they are considered to be non-polluting sources. Because of their simple structure and miniature designs, they can be placed in remote locations for remote local power compensation [2]. For continuous and versatile power generation multiple renewable sources can be connected to a single bus forming a hybrid microgrid (MG). The hybrid MG can support the local loads and also can inject power to the main grid depending on the availability of the grid [3]. With multiple renewable sources dependability on a single source can be avoided. When a single renewable source is considered, if it fails to generate power due to unavailability of natural source the load compensation is halted. Therefore, the hybrid MG can be integrated with micro-turbine wind farms, fuel-cell sources, PV plants etc [4].

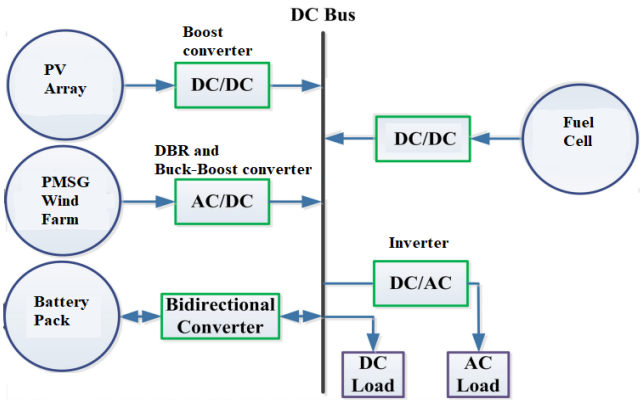

Figure 1: Schematic of hybrid renewable MG with battery backup module

Utilization of multiples renewable source connected to same bus can create stability and power quality issues and may damage the load. There must be effective solutions to overcome these issues for better stable power supply to the loads [5]. Especially in standalone hybrid renewable systems the voltage and power fluctuations are inevitable as the natural sources are unpredictable. However, the powers from the renewable sources cannot be controlled but the voltages can be stabilized using different power electronic circuits. These power electronic circuits are operated using different control algorithms ensuring maximum power extraction from the

FOREX Publication
Open Access | Rapid and quality publishing
International Journal of Electrical and Electronics Research (IJEER)
Research Article | Volume 12, Issue 2 | Pages 639-646 | e-ISSN: 2347-470X

sources [6]. For voltage stabilization along with the renewable sources, energy storage backup module like battery pack needs to be connected in parallel to the system. The controller of the battery pack converter needs to be robust to the variations caused by the renewable source due to changing environmental conditions [7]. The proposed standalone hybrid MG system with energy storage backup module supporting a local AC load can be observed in *figure 1*.

In the given schematic of the hybrid renewable MG the renewable sources considered are PV array, PMSG wind farm and Fuel-cell. These renewable sources are connected to the DC bus through unidirectional DC-DC converters. A battery pack is connected to the same DC bus through a bidirectional DC-DC converter (BDC) as the battery pack needs to be charged and discharged depending on the renewable power availability [8]. In order to stabilize the output voltage of the renewable sources converters the BDC of the battery module needs to be stable. As per the output DC voltage control of the BDC the renewable sources share power to the system. In conventional methodology as per previous researches the BDC is operated by constant voltage control with voltage value reference. The reference voltage is set as per the requirement of the system and the renewable sources capability. The duty ratio of the BDC switches is controlled by the traditional PI controller with specific integral and proportional gains tuned as per the response of the BDC. The conventional PI controller generates higher peak values and ripple in DC output voltage. This impacts the output powers of the renewable sources also. Therefore, the BDC control needs to be updated with advanced adaptive controllers for better control over the duty ratio of the switches. This improves the ripple factor and also helps to reduce the peak value and settling time of the DC link voltage. Each converter is operated by an individual controller maintaining the output DC voltage at the required value. At the load end a DC load is connected directly to the DC bus feeding from the sources directly. Whereas, the AC load is connected through a 1-ph inverter with four switches operated by Sin PWM (Pulse Width Modulation) technique. As the DC link voltage is maintained stable the AC voltage magnitude on the AC load side also maintains with stability [9]. The battery controller is updated with ANFIS controller for better stability of the DC bus voltage improving the performance of the system. This paper is organized in multiple sections with *section 1* included with introduction to the proposed system which has proposed schematic of hybrid MG. *Section 2* is the proposed hybrid MG system configuration and design of the converters of each source module. The next section 3 is the control design of the ANFIS controller integrated to battery BDC operation for better performance. The following *section 4* is the result analysis of the proposed hybrid MG system simulated with different operating conditions of the renewable sources. The results analysis validates the best controller (PI or ANFIS) for the control of the BDC in the battery module. The final conclusion to the paper with parametric analysis is done in *section 5* followed by references in the paper.

2. SYSTEM CONFIGURATION

The hybrid MG system is configured with PV source, PMSG wind farm and fuel-cell renewable sources connected to same DC bus. Along with these renewable sources an energy storage module is also connected to the DC bus for power sharing and stabilization of the system. The PV source and fuel-cell are connected with a unidirectional boost converter (BC) individually, PMSG wind farm is connected to a unidirectional buck-boost converter (BBC) [10]. The battery is integrated with a BDC which conducts power in both directions for charging and discharging of the battery pack. Two different loads, DC load and AC load are connected to the DC bus for compensation [11]. The DC load is however directly connected to the DC bus whereas the AC load is connected through a single-phase AC inverter. The complete circuit structure of the proposed hybrid MG system with all modules connected to the DC bus is shown in *figure 2*.

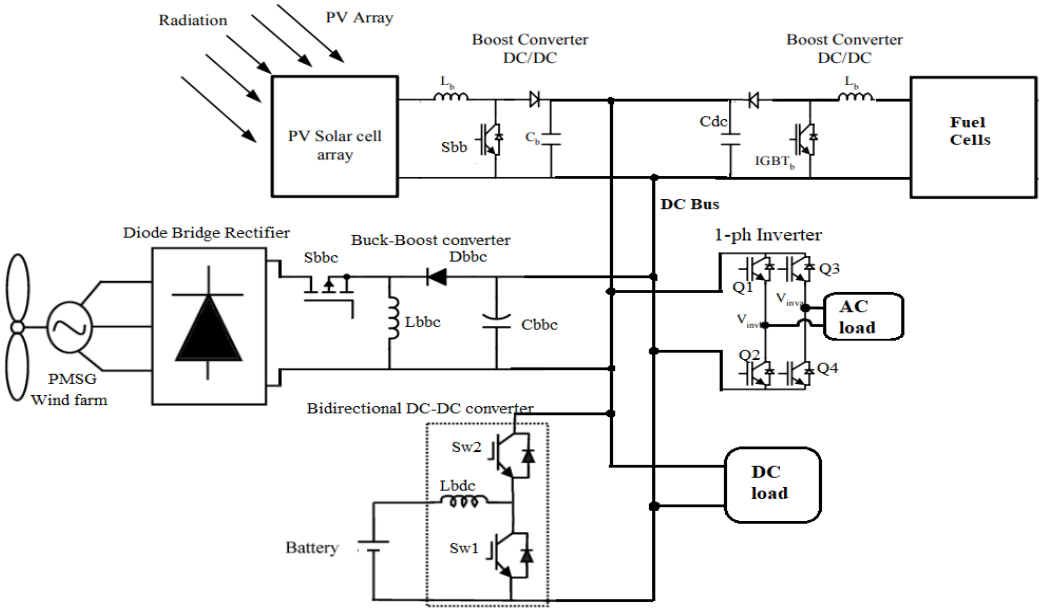

Figure 2: Proposed hybrid renewable MG system circuit structure

FOREX Publication
Open Access | Rapid and quality publishing
International Journal of Electrical and Electronics Research (IJEER)
Research Article | Volume 12, Issue 2 | Pages 639-646 | e-ISSN: 2347-470X

The BC of the PV source is controlled by Incremental Conductance MPPT (Maximum Power Point Tracking) method with feedback signals from PV source [12]. The MPPT technique determines the change in duty ratio (ΔD) of the switch in the BC. The value of the duty ratio is varied as per the change in voltage and current of the PV source (V_{pv} and I_{pv}). The rate of change of duty ratio is decided by the MPPT gain set as per the settling of the extraction from PV source.

$$D(t) = D(t-1) + \Delta D \begin{Bmatrix} If\ dV = 0\ and\ dI > 0 \\ If\ dV \neq 0\ amd\ \frac{dI}{dV} > \frac{-I_{pv}}{V_{pv}} \end{Bmatrix} \quad (1)$$

$$D(t) = D(t-1) - \Delta D \begin{Bmatrix} If\ dV = 0\ and\ dI < 0 \\ If\ dV \neq 0\ amd\ \frac{dI}{dV} < \frac{-I_{pv}}{V_{pv}} \end{Bmatrix} \quad (2)$$

Here, *dV* and *dI* are the change in voltage and current of PV source respectively, *D(t-1)* is the previous duty ratio and *D(t)* is the present duty ratio. As *D(t)* is compared to high frequency carrier sawtooth waveform generating pulses for the switch of the BC [13].

The switch in the BBC of the PSMG wind farm is controlled by power signal feedback (PSF) MPPT. The duty ratio for the switch is generated by speed (w_m) feedback from the PMSG [14]. The estimated power (P_{est}) from the PSF MPPT with 'w_m' variable is calculated as per the given expression *eq. (3)*.

$$P_{est} = K_{mppt} \cdot w_m^3 \quad (3)$$

Here, K_{mppt} is the MPPT gain of the PSF algorithm used for adjusting the P_{est} value as per the requirement. From the variable P_{est} the duty ratio D_{bbc} of the BBC is expressed in *eq. (4)*

$$D_{bbc} = (K_p + \int K_i . dt) \left(\frac{P_{est}}{w_m}\right) \quad (4)$$

The K_p K_i are the proportional and integral gains of the MPPT regulator tuned as per the response of the BBC output power. The pulse to the switch of BBC is generated by comparing the D_{bbc} with high frequency carrier waveform. The fuel cell BC and battery module BDC is controlled by constant voltage (CV) feedback control with reference value set as per the requirement at the DC bus. The expression for duty ratio (D_{fc} and D_{bdc}) of CV control operating the fuel-cell and battery module is given in *eq. (5)*.

$$D_{fc} = D_{bdc} = (K_{p\,dc} + \int K_{i\,dc} . dt)\,(V_{ref} - V_{dc}) \quad (5)$$

The values of *K_(p dc) K_(i dc)* are tuned are per the DC link voltage settling to the reference value. The fuel-cell is considered to be a backup source to the battery module. During lower State of Charge of battery (SOCbat) and battery failure conditions, the fuel-cell supports the system with the required power. During excess renewable power after the load compensation the extra power is stored into the battery [15]. During deficit renewable power conditions, the remaining load power is compensated by the fuel-cell power. The fuel-cell module is trigger ON with solar irradiation (Ir) feedback and SOCbat connected to an AND gate. The BB converter switch is triggered ON when SOCbat is below 20% and *Ir* is below 300W/mt2. The further development of the BDC control structure is discussed in next section.

3. PROPOSED CONTROL DESIGN

A As previously mentioned, the BDC of the battery module is controlled by CV control with reference DC link voltage (V_{dcref}) given as per the AC load magnitude requirement [16]. The control structure of CV controller can be seen in *figure 3*.

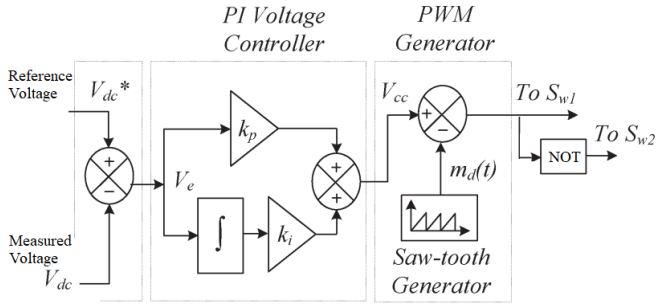

Figure 3: BDC CV control with DC voltage reference

The switches S_{w1} and S_{w2} are the high frequency operated switches of BDC which trigger alternatively with a NOT gate connected to S_{w2} switch [17]. When the duty ratio is more than 50% the BDC operates in boost mode and when it is below 50% it operates in buck mode. The boost mode makes the battery discharge and the buck mod makes the battery charge. The duty ratio (V_{cc}) value is tuned as per the PI voltage regulator gains (k_p and k_i). Due to magnifying and immediate response of the PI controller the initial peak value and oscillations in the plant are high [18]. Due to these issues the DC link voltage has high initial peak value generation and slower settling time with higher ripple content [19]. This also effects the AC voltage magnitude and the harmonic content on the load side. To mitigate these DC voltage quality issues the traditional PI controller is replaced with Adaptive Network based Fuzzy Inference System (ANFIS) [20]. The ANFIS is an advancement to the conventional Fuzzy logic control, which uses data from the PI controller input and output for training the controller. The fuzzy logic controller is set with predefined membership functions which don't change as per the input error given to the controller. As the Fuzzy control has limitation of specific range of membership functions the output is restricted to a certain range. Because of this restriction the output voltage may have higher ripple even though with lesser setting time and peak value generation. The ANFIS controller is trained as per the PI controller data which reconfigures the membership functions changing tuned as per the given input error.

This creates more control over the duty ratio signal reducing the ripple along with lower peak value generation and settling time. The *figure 4* is the structure of internal design of ANFIS controller with single input and single output design.

FOREX Publication
Open Access | Rapid and quality publishing
International Journal of Electrical and Electronics Research (IJEER)
Research Article | Volume 12, Issue 2 | Pages 639-646 | e-ISSN: 2347-470X

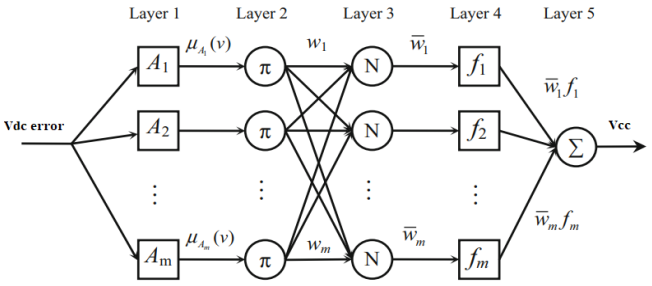

Figure 4: ANFIS internal structure

The structure of the ANFIS control is segregated into 4 layers which define the output as per the given input. The first layer is the Fuzzifier layer which provides membership functions (MFs) to the input variable (*Vdc* error). The MFs are set with 'gauss' shape and the range in determined as per the maximum and minimum error value generation [21]. The first layer is described by:

$$\mu_{A_i}(V_{dc\,error}) = gaussmf(V_{dc\,error};\ a_i, b_i, c_i) = \max\left(\min\left(\frac{V_{dc\,error}-a_i}{b_i-a_i}, \frac{c_i-V_{dc\,error}}{c_i-a_i}, 0\right)\right); \quad i = 1, 2, 3 \dots \dots . m \qquad (6)$$

The a_i, b_i, c_i determine the shape of the MF which are names as antecedent parameters. The input variable gauss type MFs with 'Sugeno' type system can be seen in *figure 5*.

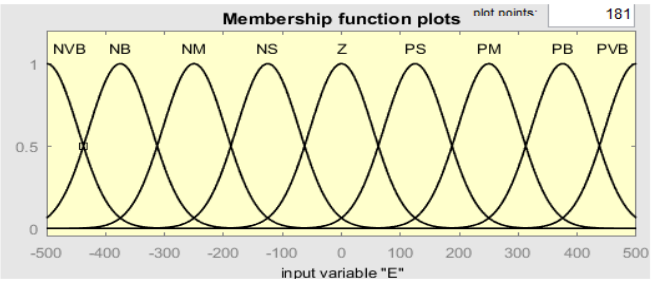

Figure 5: ANFIS Input variable MFs

The next second layer is the rules layer where the number of rules (π) will be same as number of input variable MFs. Defining the rules controls the output variable value as per the changes in the reference given by the user. The third layer is the normalizing layer which normalizes the value reducing the oscillations in the signal [22]. The normalization of the given values is defined as:

$$\overline{w_i} = \frac{w_i}{\sum_{i=1}^{m} w_i}; i = 1, 2, 3 \dots \dots, m \qquad (7)$$

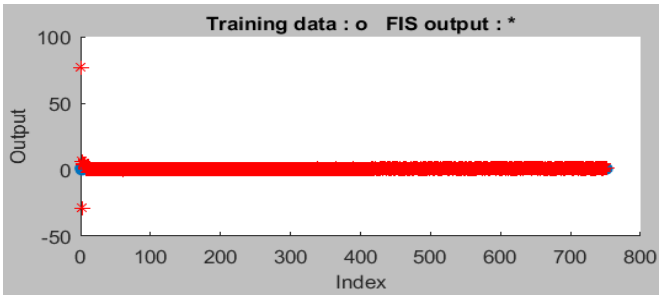

Figure 6: ANFIS data training

The normalization is done by training the ANFIS MFs as per the input and output data of the PI controller with 'back-propagation' optimization technique [23]. The trained data with the previous data obtained by the ANFIS tool can be observe in *figure 6*.

The fourth layer is Defuzzifier layer which is defined by multiplication of normalized variable with a polynomial generating final signals given as in (8).

$$\overline{w_i}.f_i = \overline{w_i}\ (k_i V_{dc\,error} + r_i);\ i = 1, 2, 3 \dots \dots, m \qquad (8)$$

The final layer is the summation layer which is determined by the summation of all the signals received after fourth layer given as:

$$\sum_{i=1}^{m} \overline{w_i}.f_i = \frac{\sum_{i=1}^{m} \mu_{A_i}(V_{dc\,error})(k_i V_{dc\,error} + r_i)}{\sum_{i=1}^{m} \mu_{A_i}(V_{dc\,error})}; i = 1, 2, 3 \dots \dots, m \qquad (9)$$

The final values received from the ANFIS controller is compared to high frequency sawtooth generator for generation of pulses to BDC switches S_{w1} and S_{w2}. The ANFIS controller is a complex controller which needs rigorous training and data from previous controller. The only possible optimization techniques are restricted to only two types which are 'back-propagation' and 'hybrid' algorithms. The membership functions are trained with either of these two algorithms and the better one needs to be selected for the plant.

4. RESULT ANALYSIS

This The proposed hybrid renewable MG with three renewable sources (PV source, wind farm, fuel-cell) and one energy storage module (battery module) is modeled in MATLAB Simulink tool.

Table 1: Configuration parameters

Name of the module	Parameters
PV source	PV Manufacturer: SunPower SPR-X20-250-BLK-A-AC, V_{mp}=42.8V, I_{mp}=5.84A, V_{oc}=50.93V, I_{sc}=6.2A, N_s=5, N_p=50, P_{pv}=62.5kW. Boost converter: L_b=1mH, C_{in}=100uF, R_{igbt}=1mΩ, f_s=5kHz.
PMSG wind farm	PMSG: Rs=0.0005Ω, Ls=0.0935mH, φ=0.153V.s, J=20, F=0.1889, P=4, wm_{int}=314.15rad/sec. Turbine: P_n=70kW, base wind speed: 12m/s, Maximum power at base wind speed=1pu. Buck-Boost converter: L_{bb}=100uH, C_{in}=1000uF, R_{igbt}=1mΩ, f_s=5kHz.
Fuel-Cell	V_{nom}=300V, I_{nom}=80A, V_{end}=125V, I_{end}=280A. Boost converter: L_b=1mH, C_{in}=100uF, R_{igbt}=1mΩ, f_s=5kHz, $V_{dc\,ref}$=380V.
Battery	V_{nom}=200V, Capacity=200Ah, SOC_{int}=50% BDC: L_{bdc}=1mH, R_{igbt}=1mΩ, f_s=5kHz, $V_{dc\,ref}$=380V.
Inverter and AC load	Single phase full bridge four IGBT switch inverter: $V_{dc\ bus}$ = 400V, R_{igbt}=1mΩ, L_f=1mH, C_f=100uF, f_s=5kHz, m=0.99, P_{load}=100kW at 230V_{rms}.

FOREX Publication
Open Access | Rapid and quality publishing
International Journal of Electrical and Electronics Research (IJEER)
Research Article | Volume 12, Issue 2 | Pages 639-646 | e-ISSN: 2347-470X

All the blocks for modeling of the system are considered from 'Power system' toolbox of the Simulink library. The controllers are modelled as per the measurements taken as feedback from the source blocks controlling the switches of the power electronic circuits. The complete configuration parameters of the hybrid renewable MG is given in *table 1*.

As per the given parameters in *table 1* the simulation model is updated and is simulated with different operating conditions. The operating conditions are created by varying the solar irradiation and wind speed at different instants of time. The graphs of each variable measured from the source modules are recorded and plotted with time as reference. A comparative graph plotting is done with conventional PI and ANFIS controllers integrated in BDC controller of the battery module with same operating conditions. The simulation results are validated with comparison of different parameters of the measured signals determining the best controller. The simulation is run for 6s with operating conditions set with two cases, with graphs plotted accordingly.

Case 1: Irradiation changed from 1000W/mt2 to 200W/mt2 at 2s, Wind speed changed from 12m/s to 8m/s at 4s, Battery initial SOC at 80%.

The solar irradiation, wind speeds and battery initial SOC are set as per the given conditions in *case 1* and the simulation is run for 6s. The *figure 7* has the graphs generated for all the modules powers and DC link voltage for *case 1*.

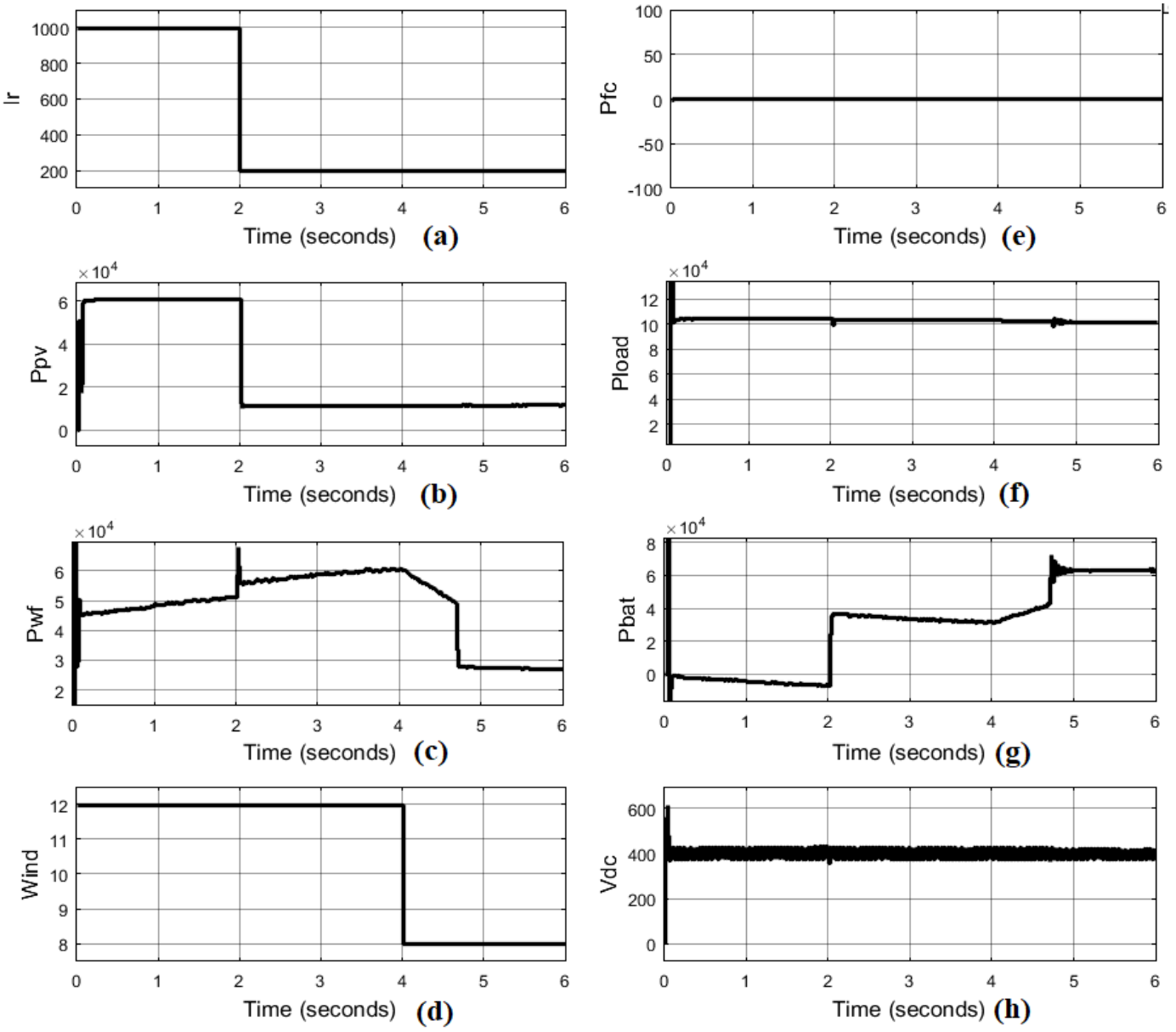

Figure 7: (a) Solar irradiation (Ir) (b) Active power of PV source (Ppv) (c) Active power of wind farm (Pwf) (d) Wind speed (m/s) (e) Active power of fuel-cell (f) Active power of load (g) Active power of battery pack (h) DC link voltage for *case 1*

FOREX Publication
Open Access | Rapid and quality publishing
International Journal of Electrical and Electronics Research (IJEER)
Research Article | Volume 12, Issue 2 | Pages 639-646 | e-ISSN: 2347-470X

The PV power in *figure 7(a)* initially is at 60kW which is dropped to 12kW at 2s when the *Ir* is dropped. The wind farm power in *figure 7(c)* generates 50 – 60kW when the wind speed is at 12m/s and drops to 28kW when the wind speed drops to 8m/s at 4sec. As the SOC of the battery is above 20% the fuel-cell module is not activated and the fuel-cell power in *figure 7(e)* is at '0'. As in *figure 7(g)* battery initially charges with 5kW until 2s later discharges with 40kW as *Ir* drops. When the wind speed is dropped at 4s the discharge power of the battery is increased to 60kW compensating the load with full power of 100kW. As observed in *figure 7(f) and 7(h)* for any given condition the load power is maintained at 100kW and DC link voltage at 400V throughout the simulation.

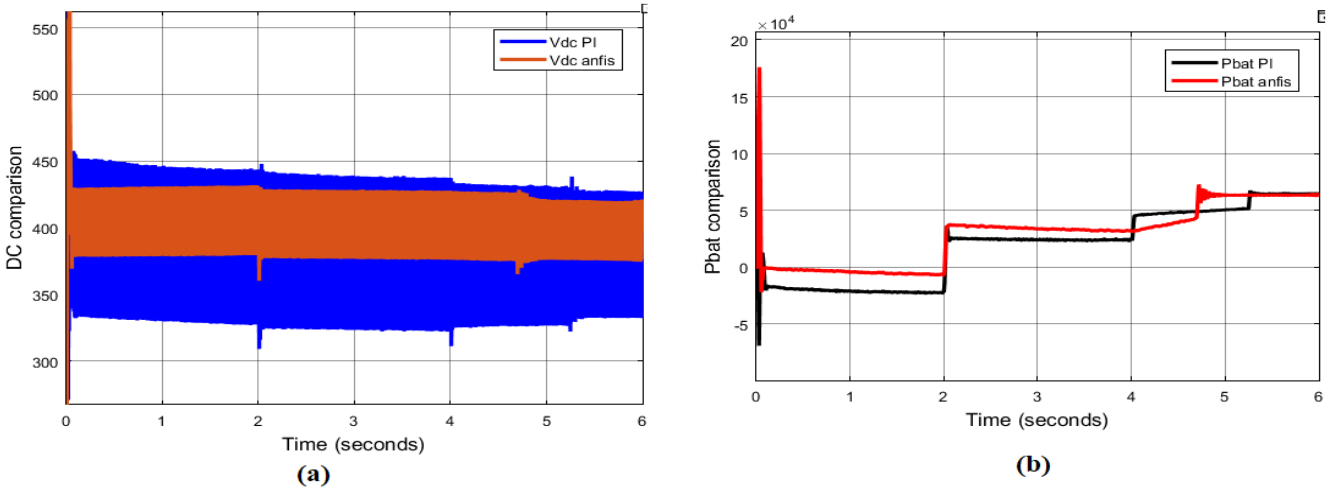

Figure 8: (a) DC link voltage comparison (b) Battery power for *case 1*

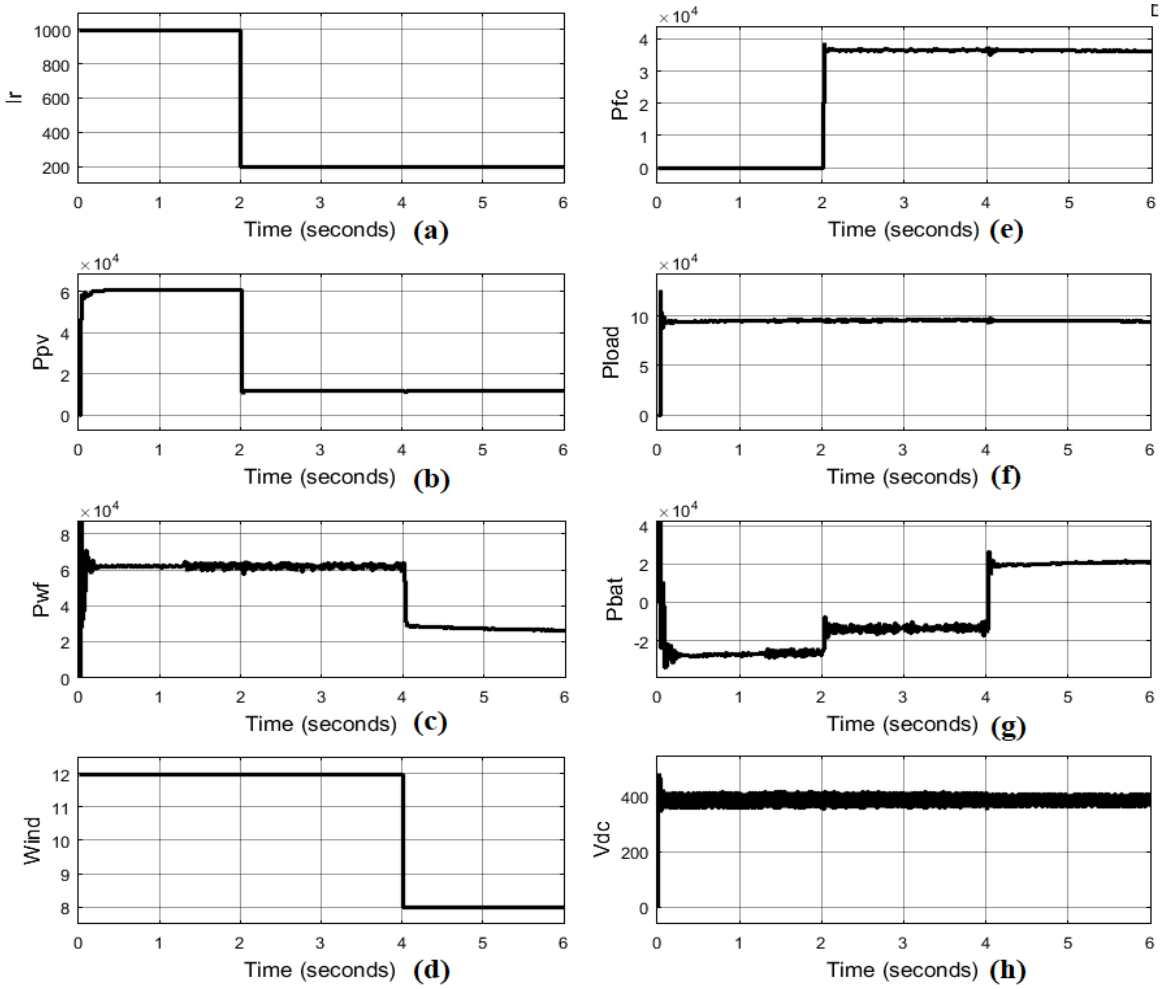

Figure 9: (a) Solar irradiation (Ir) (b) Active power of PV source (Ppv) (c) Active power of wind farm (Pwf) (d) Wind speed (m/s) (e) Active power of fuel-cell (f) Active power of load (g) Active power of battery pack (h) DC link voltage for case 2

FOREX Publication
Open Access | Rapid and quality publishing
International Journal of Electrical and Electronics Research (IJEER)
Research Article | Volume 12, Issue 2 | Pages 639-646 | e-ISSN: 2347-470X

Similar to case 1 the PV power drops from 60kW to 12kW at 2s and wind farm power drops from 60kW to 28kW at 4s with variation in *Ir* and wind speed. But in case 2 as the SOC of the battery is low, the fuel cell provides 36kW power to the load from 2s. Initially the battery charges with a power of 30kW as the initial SOC is low. Later as the load demand is higher than the fuel cell capacity, the battery discharges with only 20kW at 4s.

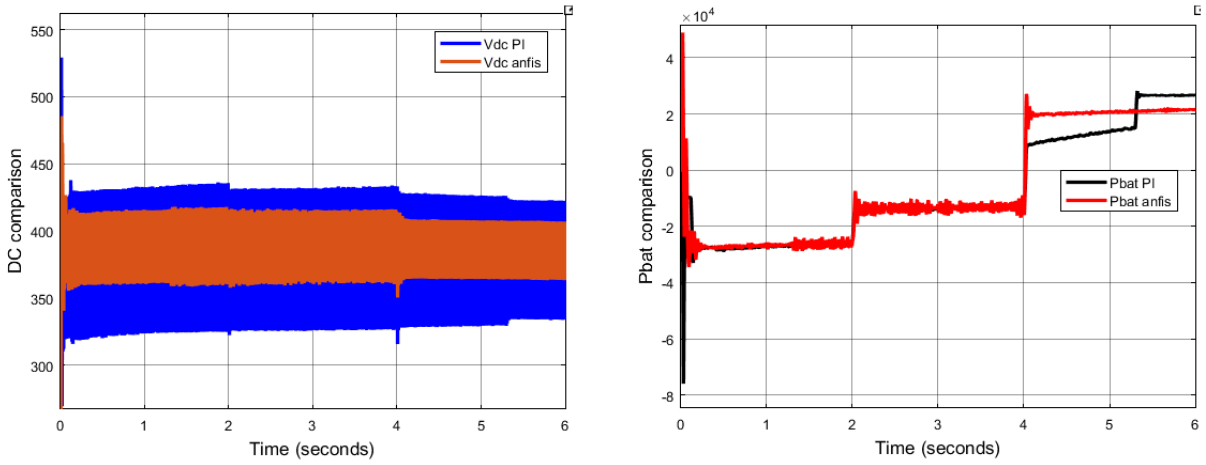

Figure 10: a) DC link voltage comparison b) Battery powerfor case 2

As observed in *figure 10a* the DC link voltage has less ripple content with the system is updated with ANFIS controller. The battery power in *figure 10b* is more stable and has lesser discharge, as during lower renewable power conditions the fuel-cell supports the load. As per the given graphs a parametric comparison table is given in *table 2* validating the better controller.

Table 2: Comparison table

Name of the parameter	PI	ANFIS
Vdc ripple	30.5%	14.9%
Vdc peak	530V	480V
Pbat	27kW	20kW
Pbat peak	75kW	34kW

5. CONCLUSION

The modeling of a standalone hybrid renewable MG with energy storage module and a backup renewable power module (fuel cell) is done. Unpredictable renewable sources PV and wind farm are operated by MPPT algorithm for maximum power extraction. As the MG is isolated from the main grid a battery module is connected to the DC bus supporting the load. The battery module also has the capability to store excess renewable power from PV and wind farm. The system is operated at different SOC of the battery to determine the stability of the system for the environmental effects on PV and wind farm. It is observed that during high battery SOC conditions the battery module supports the load when the renewable power drops. Whereas, during low battery SOC the backup renewable source fuel-cell supports the load during lower PV and wind farm power generation. A comparative analysis is done on the system DC link and battery power with conventional PI and ANFIS controller by plotting overlapping graphs. As per comparison table when the battery control is updated with ANFIS training done by the data provided by the previous PI controller, the ripple and the peak values of the DC voltage and battery power are reduced to an extent. The DC voltage ripple has dropped to 14.9% from 30.5% and the peak values of the battery power is reduced to 34kW from 75kW. These two parametric comparisons determine that the ANFIS controller is considered to be an advancement to the standalone hybrid renewable MG improving its performance.

REFERENCES

[1] O. M. Babatunde, J. L. Munda and Y. Hamam, "A Comprehensive State-of-the-Art Survey on Hybrid Renewable Energy System Operations and Planning," in IEEE Access, vol. 8, pp. 75313-75346, 2020, doi: 10.1109/ACCESS.2020.2988397.

[2] S. M. Dawoud, X. Lin, M. I. Okba, Hybrid renewable microgrid optimization techniques: A review, Renewable and Sustainable Energy Reviews 82 (2018) 2039–2052 (2018).

[3] Y. Jiang, C. Wan, C. Chen, M. Shahidehpour and Y. Song, "A Hybrid Stochastic-Interval Operation Strategy for Multi-Energy Microgrids," in IEEE Transactions on Smart Grid, vol. 11, no. 1, pp. 440-456, Jan. 2020, doi: 10.1109/TSG.2019.2923984.

[4] M Jayachandran, G Ravi, Design and Optimization of Hybrid Micro-Grid System, Energy Procedia, Volume 117, 2017, Pages 95-103, ISSN 1876-6102, https://doi.org/10.1016/j.egypro.2017.05.111.

[5] C. G. Monyei, A. O. Adewumi, D. Akinyele, O. M. Babatunde, M. O. Obolo, J. C. Onunwor, A biased load manager home energy management system for low-cost residential building low-income occupants, Energy 150 (2018) 822–838 (2018).

[6] Kharrich, M.; Kamel, S.; Alghamdi, A.S.; Eid, A.; Mosaad, M.I.; Akherraz, M.; Abdel-Akher, M. Optimal Design of an Isolated Hybrid Microgrid for Enhanced Deployment of Renewable Energy Sources in Saudi Arabia. Sustainability 2021, 13, 4708. https://doi.org/10.3390/su13094708.

[7] C. Huang, H. Zhang, Y. Song, L. Wang, T. Ahmad and X. Luo, "Demand Response for Industrial Micro-Grid Considering Photovoltaic Power Uncertainty and Battery Operational Cost," in IEEE Transactions on Smart

International Journal of
Electrical and Electronics Research (IJEER)
Research Article | Volume 12, Issue 2 | Pages 639-646 | e-ISSN: 2347-470X

Grid, vol. 12, no. 4, pp. 3043-3055, July 2021, doi: 10.1109/TSG.2021.3052515.

[8] Amar Kumar Barik, Smriti Jaiswal & Dulal Chandra Das (2022) Recent trends and development in hybrid microgrid: a review on energy resource planning and control, International Journal of Sustainable Energy, 41:4, 308-322, DOI: 10.1080/14786451.2021.1910698.

[9] Saponara, S.; Saletti, R.; Mihet-Popa, L. Hybrid Micro-Grids Exploiting Renewables Sources, Battery Energy Storages, and Bi-Directional Converters. Appl. Sci. 2019, 9, 4973. https://doi.org/10.3390/app9224973.

[10] X. Ma, S. Liu, H. Liu and S. Zhao, "The Selection of Optimal Structure for Stand-Alone Micro-Grid Based on Modeling and Optimization of Distributed Generators," in IEEE Access, vol. 10, pp. 40642-40660, 2022, doi: 10.1109/ACCESS.2022.3164514.

[11] Y. Liang, H. Zhang, M. Du and K. Sun, "Parallel coordination control of multi-port DC-DC converter for stand-alone photovoltaic-energy storage systems," in CPSS Transactions on Power Electronics and Applications, vol. 5, no. 3, pp. 235-241, Sept. 2020, doi: 10.24295/CPSSTPEA.2020.00020.

[12] Pires, V.F.; Pires, A.; Cordeiro, A. DC Microgrids: Benefits, Architectures, Perspectives and Challenges. Energies 2023, 16, 1217. https://doi.org/10.3390/en16031217

[13] W. Jiang, C. Yang, Z. Liu, M. Liang, P. Li and G. Zhou, "A Hierarchical Control Structure for Distributed Energy Storage System in DC Micro-Grid," in IEEE Access, vol. 7, pp. 128787-128795, 2019, doi: 10.1109/ACCESS.2019.2939626.

[14] Babangida Modu, Md Pauzi Abdullah, Mufutau Adewolu Sanusi, Mukhtar Fatihu Hamza, DC-based microgrid: Topologies, control schemes, and implementations, Alexandria Engineering Journal, Volume 70, 2023, Pages 61-92, ISSN 1110-0168, https://doi.org/10.1016/j.aej.2023.02.021.

[15] Rangarajan, S.S.; Raman, R.; Singh, A.; Shiva, C.K.; Kumar, R.; Sadhu, P.K.; Collins, E.R.; Senjyu, T. DC Microgrids: A Propitious Smart Grid Paradigm for Smart Cities. Smart Cities 2023, 6, 1690-1718. https://doi.org/10.3390/smartcities6040079.

[16] Yang, Z.; Wang, C.; Han, J.; Yang, F.; Shen, Y.; Min, H.; Hu, W.; Song, H. Analysis of Voltage Control Strategies for DC Microgrid with Multiple Types of Energy Storage Systems. Electronics 2023, 12, 1661. https://doi.org/10.3390/electronics12071661

[17] A. F. Habibullah and K. -H. Kim, "Decentralized Power Management of DC Microgrid Based on Adaptive Droop Control with Constant Voltage Regulation," in IEEE Access, vol. 10, pp. 129490-129504, 2022, doi: 10.1109/ACCESS.2022.3228703.

[18] Magaldi, G.L.; Serra, F.M.; de Angelo, C.H.; Montoya, O.D.; Giral-Ramírez, D.A. Voltage Regulation of an Isolated DC Microgrid with a Constant Power Load: A Passivity-based Control Design. Electronics 2021, 10, 2085. https://doi.org/10.3390/electronics10172085

[19] Md. Shafiul Alam, Fahad Saleh Al-Ismail, Fahad A. Al-Sulaiman, Mohammad. A. Abido, Energy management in DC microgrid with an efficient voltage compensation mechanism, Electric Power Systems Research, Volume 214, Part A, 2023, 108842, ISSN 0378-7796, https://doi.org/10.1016/j.epsr.2022.108842.

[20] Alice Hepzibah, A., Premkumar, K. ANFIS current–voltage controlled MPPT algorithm for solar powered brushless DC motor-based water pump. Electr Eng 102, 421–435 (2020). https://doi.org/10.1007/s00202-019-00885-8

[21] S. Fathima and U. Syamkumar, "ANFIS driven DC Link Voltage Control and Power Quality Enhancement in PV-Battery Incorporated UPQC," 2022 IEEE 3rd Global Conference for Advancement in Technology (GCAT), Bangalore, India, 2022, pp. 1-6, doi: 10.1109/GCAT55367.2022.9971866.

[22] J. Saroha, M. Singh and D. K. Jain, "ANFIS-Based Add-On Controller for Unbalance Voltage Compensation in a Low-Voltage Microgrid," in IEEE Transactions on Industrial Informatics, vol. 14, no. 12, pp. 5338-5345, Dec. 2018, doi: 10.1109/TII.2018.2803748.

[23] Srimatha, S., Mallala, B. & Upendar, J. A novel ANFIS-controlled customized UPQC device for power quality enhancement. Journal of Electrical Systems and Inf Technol 10, 55 (2023). https://doi.org/10.1186/s43067-023-00121-1.